Design and Analysis of Single-phase Adaptive Passive Part coupling Hybrid Active Power Filter (HAPF)

Lei Wang[1], Ying Pang[1], Chi-Seng Lam[2], Jian-Yang Deng[1,2] and Man-Chung Wong[1,2]
1 - Department of Electrical and Computer Engineering, Faculty of Science and Technology, University of Macau, Macau, China
2 - State Key Laboratory of Analog and Mixed-Signal VLSI, University of Macau, Macau, China
E-mail: cslam@umac.mo / C.S.Lam@ieee.org

***Abstract*—In this paper, a new structure of a single-phase hybrid active power filter (HAPF) with adaptive passive part and active part is proposed. The HAPF as a state-of-the-art power quality compensator is combining the advantage of passive filter and active filter. However, it may still suffer the high initial and operational costs situation under the capacitive load case. With the proposed topology, the reactive power and harmonics of the loading can be compensated dynamically. The structure can be applied to general household appliances including inductive and capacitive loading. Compared with the traditional APF for inductive loading compensation and HAPF for capacitive loading compensation, the proposed HAPF requires a low dc-linked voltage under both inductive and capacitive loading compensation, which can reduce the initial and operational costs. Especially, the transient condition has been analyzed when the passive part is switched to verify the feasibility of this topology. Finally, representative simulation and experimental results are presented to prove the compensation effect of this single-phase HAPF with adaptive passive part.**

Index Terms—Adaptive passive part, Hybrid active power filter (HAPF), DC-link voltage, Low cost;

I. INTRODUCTION

In contemporary society, with the proliferation of power electronics equipment and switching devices, it is getting more difficult for the electric utility to supply its customers with a sinusoidal voltage and current within an acceptable tolerance [1]. Basically, the great increase usage of nonlinear loads can produce reactive power, harmonic currents and neutral current problems, which consequently distort the voltage waveform. Therefore, the research of power quality issues has captured exponentially increasing attention in the power engineering community in the past decades [2] –[11]. From that time, different power quality compensators have been proposed successively.

At the beginning, capacitor banks (CBs), passive power filter (PPFs) have been proposed to compensate the reactive power and harmonic [2] –[5]. Due to its economical efficiency, these fixed passive compensators have been applied successfully. However, with the development of the demand of the request of power quality and the increase number of complex load. These compensators cannot satisfy the requirement. Thus, active power filer (APF) has been present. Because it can compensate the power quality based on the load conditions, APF brought many benefits to power system and it can be installed in different conditions. On the other hand, due to the initial costs and running costs of the APF, APF cannot be applied massively [2], [3], [7]–[13]. To overcome the shortages of APF, the hybrid active power filters (HAPFs) were proposed. The HAPF uses the passive elements to reduce the ratings of the costly active part. In [5]–[7], the passive part of HAPF is designed to minimizing the ratings of the active part so as to reduce the cost of the whole system under the inductive loading. Usually, the passive part in HAPF is fixed and cannot adapt the changing of the loads [4], [5] which may bring the loss when the passive part cannot fit the load, for example when the load is capacitive, the HAPF need produce more inductive current to compensate than APF. As a result, the research direction of the passive part should be adjusted accordingly and subjected to the dynamical loads.

Therefore, this paper aims to:

- Propose the passive part of the HAPF design method according to the compensation range analysis;
- Analysis the transient problems during the dynamic load changing and avoid the transient effect caused by the change-over between each passive component are proposed;
- Propose adaptive passive part of HAPF with the functions of enlarge compensation range of traditional HAPF while keeping a low operating dc-link voltage.

The layout of this paper is given as follows. In section II, the structure of HAPF with adaptive passive part is proposed to adapt different load conditions. A realistic power using condition is set as analysing example. Based on that, the passive part of the HAPF can be designed according to the compensation range analysis. In section III, the transient problems during the dynamic load changing will be analysed and solutions for avoid the transient effect caused by the

Project Supported in part by the Science and Technology Development Fund, Macao SAR (FDCT) (025/2017/A1, 109/2013/A3) and in part by the Research Committee of the University of Macau (MYGR2017-00038-FST, MYRG2015-00009-FST and MYRG2017-00090-AMSV)

change-over between each passive component are proposed. In section IV, the detail in control of mode selecting and best switches turning time is going to be decided Then, the simulation and experimented results are provided in section V and VI to verify the proposed the adaptive HAPF for reactive power and harmonics current compensation Finally, the conclusion is drawn in section VII.

II. The Design Method of Adaptive Passive Part of HAPF

A. Structure of Adaptive Passive Part of HAPF

The design of HAPF with adaptive passive part need to ensure the nonlinear load can be compensated under both inductive load and capacitive load with a relatively low DC-link voltage level, so the following structure shown in Fig. 1 combing APF and HAPF together to fulfill the target.

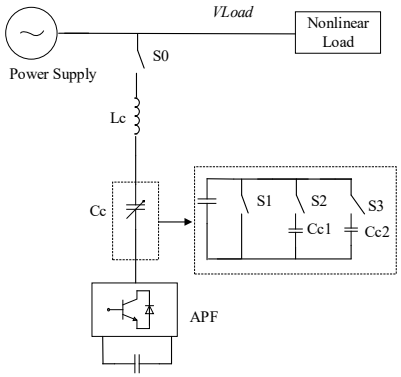

Fig. 1. Structure of designed HAPF with adaptive passive part

In Fig. 1, S_1,S_2,S_3 are three controllable switches, which are controlled based on the load condition. L_C and C_C are coupling inductor and capacitor which is an adaptive capacitor. For the controllable part, the control block is shown in Fig. 2.

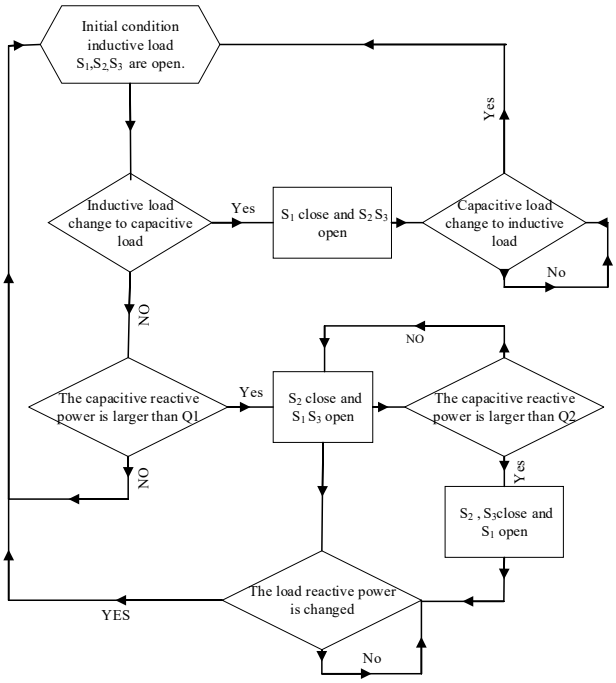

Fig. 2 The control block of adaptive capacitor in HAPF

With the control block, the controller can choose the mode automatically to fit the load conditions. In traditional HAPF structure, coupling *LC* structure is fixed, when the load is capacitive the active part of HAPF has to produce more inductive current, which means the dc-link voltage needed is higher than the traditional one and high-cost. Thus, the adaptive capacitor is designed to fit different load conditions. As for the value of the capacitor and the inductor, the value is determined and designed by the using environment. In this paper, the environment is mainly focused on low-dc system and home use environment. After the parament of power quality is obtained, the design can be started based on the statics.

B. Design of the passive part of HAPF

The main purpose of the passive part of the HAPF is to compensate the loading reactive power load consumption. In this design, ideally the reactive power fully compensated by passive part components, the fundamental load reactive power Q_{Lf} and compensating reactive power Q_{PF} have the same magnitude and opposite direction under the inductive load case.

$$Q_{Lf} + Q_{PF} = 0 \tag{1}$$

The passive filter fundamental relative power Q_{PF1} generation can be expressed as[5] :

$$Q_{PF1} = \left(\frac{\omega C_C}{\omega^2 L_C C_C - 1} \right) V_L^2 \tag{2}$$

where L_c means the value of coupling inductor; C_C is the value of coupling capacitor and $\omega=2\pi f$. Thus, the coupling capacitor C_C can be expressed as[7] :

$$C_C = \frac{I_{Lf} \sin\theta_{Lf}}{\omega\left(I_{Lf} \sin\theta_{Lf} \omega L_C + V_L\right)} \tag{3}$$

The purpose of L_C mainly is to eliminate the harmonics which is produced by the active part of HAPF due to the turn-on and turn-off of the power switches devices. The value of the L_C can be expressed as [11] :

$$L_C \geq \frac{V_{DC}}{8 \cdot f_s \cdot \Delta i_{L_C \max}} \tag{4}$$

where, V_{DC} is the dc-link voltage, f_s is the switching frequency, $\Delta i_{L_C \max}$ is the maximum allowed output current ripple value. Therefore, all of L_C and C_C can be calculated. As for the V_{DC} is determined by the current which is produced by the inverter, and the equation can be expressed by

$$V_{DC} = \sqrt{\sum_{n=2}^{\infty} V_{dcn}^2 + V_{dcre}^2} \tag{5}$$

where $V_{dcre} = \sqrt{6} V_x \times \left| 1 - \frac{Q_{Load}}{Q_{LC}} \right|$ and $V_{dcn} = \sqrt{6} \left| n2\pi fL + \frac{1}{n2\pi fC} \right| |I_n|$

The values of the parameters in the adaptive HAPF can be selected in this paper based on the characteristics of the loads shown before. Parameters under inductive loading case will be obtained. Based on a realistic example of power using example, the conditions can be drafty divided according to the

amount of reactive power need to be compensated as shown in Table I.

TABLE I THE DIVIDED LOAD LEVELS BASED ON COMPENSATED REACTIVE POWER

Level	Inductive load level 1	Inductive load level 2	Inductive load level 3	Inductive load level 4
Reactive Power (VAR)	250< Q<750	750< Q<1250	1250< Q<1750	1750< Q<2250

As a result, the corresponding capacitance and inductance in this paper is calculated as followed.

TABLE II THE COMPENSATED REACTIVE POWER AND THE CORRESPONDING CAPACITANCE AND INDUCTANCE

Level (inductive)	level 1	level 2	level 3
Reactive Power _Best case	633.54 VAR	1269.07VAR	1900.61VAR
Coupling Capacitance	40μF	80μF	120μF
Coupling Inductive	10mH	10mH	10mH

III. TRANSIENT STUDY OF ADAPTIVE PASSIVE PART OF HAPF

Refer to the design structure as shown in Fig. 1, there may be large transient problems occurring in system if the switches are not turned on/off at the proper time. In order to avoid the transient problems, all of the possible transient equations are deduced and the ideal switch turning on/off time can be found to find the time point of minimum transient current. There are totally 4 categories of transient situation will be contained in the designed system, namely, a) Start-up transient; b) inductive load transient when load changed; c) transient analysis when capacitive load change to inductive load; d) transient analysis when inductive load change to capacitive load.

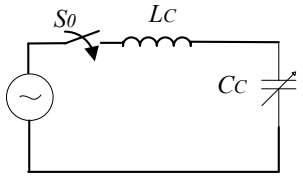

Fig. 3 Simplified model of the start-up transient

The simplified model of condition a) is shown in Fig. 3, the switch S_0 is set to be open before it is being used. In this situation, there are two conditions need to be satisfied before starting the adaptive HAPF, namely, 1) The dc link voltage V_{dc} at the low level or equal to zero and 2) Capacitor voltage equal to zero V_{Cc}=0. The simplified model of the start-up transient is further mortified as Fig. 3.

According to basic circuit analysis theory, the differential equation shown in Fig. 3 can be deduced as:

$$L_C \frac{di}{dt} + \frac{1}{C_C}\int_0^t i\,dt = v \tag{6}$$

After mathematics calculation, the transient equation of inductor current can be obtained as below:

$$i = -\frac{V_m \omega C_C}{1 - L_C C_C \omega^2}\sin(\omega t + \phi) + \frac{V_m \cos(\phi) C_C}{\sqrt{L_C C_C}\left(1 - L_C C_C \omega^2\right)}\sin\left(\frac{1}{\sqrt{L_C C_C}}t\right) + \frac{V_m \omega C_C \sin(\phi)}{1 - L_C C_C \omega^2}\cos\left(\frac{1}{\sqrt{L_C C_C}}t\right) \tag{7}$$

where, the transient voltage of the power supply is expressed as $v = V_m \cos(\omega t + \phi)$

The worst-case situation during start-up process is based on the magnitude of capacitor voltage and inductor current. For minimum case, the switch will be turned on at $\phi = \pm\frac{n\pi}{2}$ which is the zero point of the load voltage. While for the worse case, the switch will be turned on at $\phi = \pm n\pi$,where n= 1, 2, 3…. And these are the maximum point of the load voltage.

For condition b) to e), the mathematics calculation progress is used the same circuit theory Kirchhoff voltage law (KVL) and the solution of second order differential equation the following results can be obtained.

TABLE III THE BRIEF SUMMARY OF THE TRANSIENT SITUATIONS

Switch No.	Best Switch Turn-on Time	Best Switch Turn-off Time
S_0	Zero load Voltage V_{Load}=0V and Zero capacitor voltage V_{cc}=0V	No limitations
S_1	Zero capacitor Voltage V_{cc}=0V	No limitations
S_2	Zero capacitor Voltage V_{cc}=0V	Zero capacitor Voltage V_{cc}=0V
S_3	Zero capacitor Voltage V_{cc}=0V	Zero capacitor Voltage V_{cc}=0V

IV. MODE SELECTING AND BEST SWITCHES TURNING TIME

The reasonable structure of HAPF is chosen for a single-phase system, which combines the adaptive passive part and controllable active part. Based on the pervious fundamental reactive power compensation's discussion, it found that the structure of HAPF can reduce the dc-linked voltage under inductive load case, while the APF is more suitable for capacitive load case.

The circuit structure and control block of passive part are shown in Fig. 1 and Fig. 2 separately. The system parameters after calculated is shown as below.

TABLE IV CALCULATED SYSTEM PARAMETERS FOR DIFFERENT CASES

System Parameters	Physical Values
V_L (RMS) , V_{dc}	220 V,
I_L (RMS), THD_{iL}	Varying, 30%
Lc, Cc, C_{c1}, C_{c2}	*10mH, 40μF,40μF, 40μF*

According there two considerations, the programming of passive switches control can be drafty divided into two parts, namely a) Best switches turning time obtaining and b) Mode selecting.

A. Best switches turning time obtaining

The trigger signals obtained only according to the load reactive power cannot be treated as the final switch driving signals. However, if the best switches turning conditions are combined with the trigger signals obtained from Q_{Load}, the whole control programming of passive switches can be obtained.

According to the transient analysis in section III. , the switches have the best turning on/off time which can minimize the transient problems. From Table III, it can be clearly seen that the designed switch turn on/off times are related to zero *Vcc, Ic,* $V_{Load.}$, the trigger ranges of the *Vcc, Ic ,* V_{Load} are listed in Table V.

TABLE V THE TRIGGER RANGES OF THE *VCC, IC ,V_{LOAD}*

Trigger component	*Vcc,*	*Ic*	V_{Load}
Trigger Ranges	*-2V<Vcc<2V*	*0.01A<Vcc<0.01A*	*-2V<Vcc<2V*

The process chart and the waveform illustrations of obtaining the best switch driving signals are shown in Fig. 4 (a) and (b).

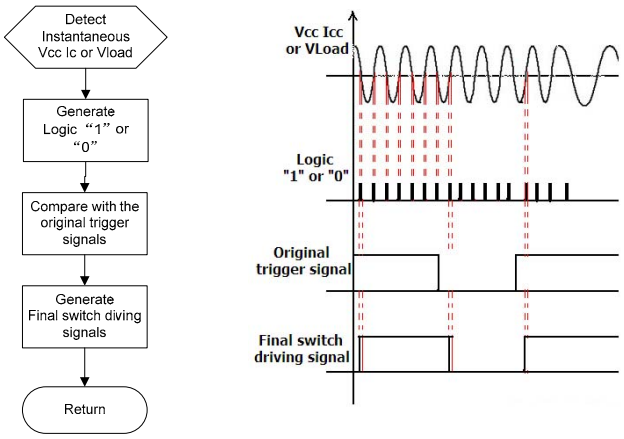

(a) (b)

Fig. 4 (a) process chart of the obtaining the best switch driving signals; (b) corresponding waveform illustration of the obtaining the best switch driving signals

B. Mode selecting

According to the previous discussion, the different modes with corresponding load reactive power ranges table and the flowchart in can be obtained.

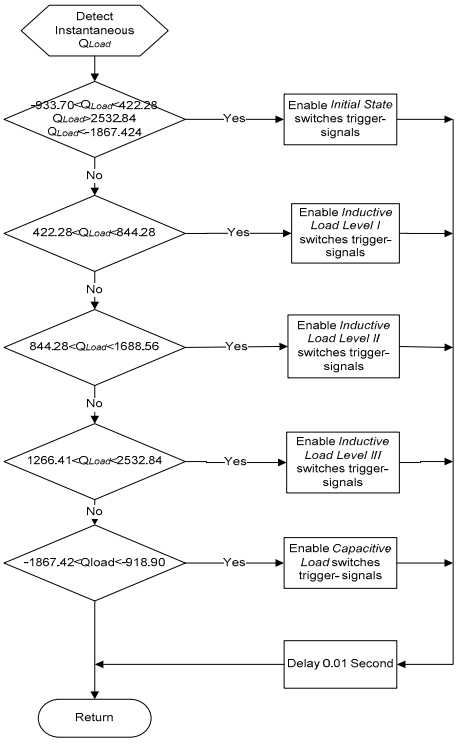

Fig. 5 The routine of mode section

TABLE VI THE DIFFERENT MODES WITH CORRESPONDING LOAD REACTIVE POWER RANGES

Mode	Range of Q_{Load}*(VAR)*	Mode	Range of Q_{Load} *(VAR)*
Inductive load level 1	422.28< *Q*<844.28	Capacitive load	-1867.42< *Q*<-933.70
Inductive load level 2	844.28 < *Q*<1688.56	Initial State	-933.70< *Q*< 422.28 *Q*>2532.84 and *Q*< -1867.42
Inductive load level 3	1266.41< *Q*<2532.84		

V. SIMULATION RESULT

The overall simulation need cover all the types of transient situations. Therefore, time steps of the overall transients can be listed as shown in Table VII and the setting of the simulation is shown in Table IV.

TABLE VII TIME STEPS OF THE OVERALL TRANSIENT

Period	Mode of compensator	Types of transient
0-1s	Initial state	
1-2s	Inductive load level 1	Start up transient
2-3s	Inductive load level 2	Inductive load transient- more inductive load are added
3-4s	Inductive load level 1	Inductive load transient- part of inductive load are taken out
4-5s	Capacitive load	Capacitive load change to inductive load
5-6s	Inductive load level 1	Inductive load change to capacitive load
6-7s	Initial state	Close off transient

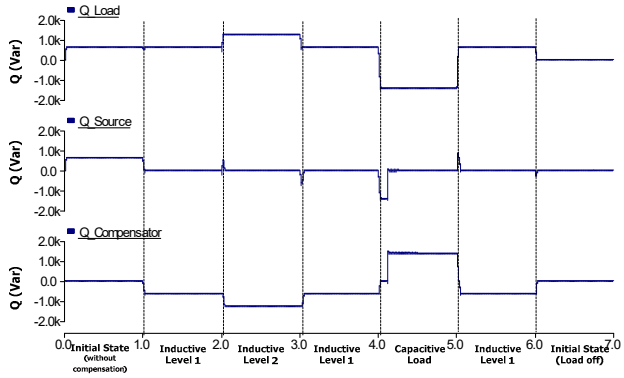

Fig. 6 Dynamic reactive power diagram

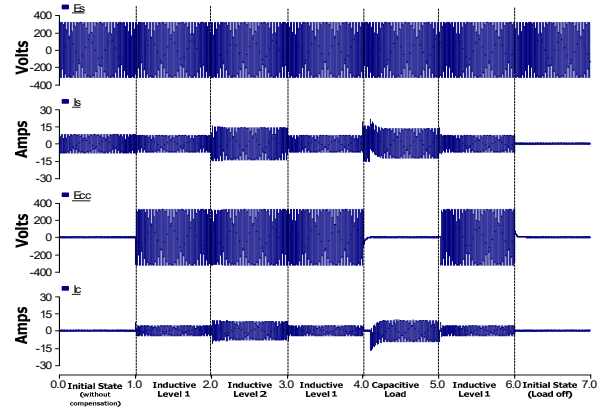

Fig. 7 Dynamic waveforms of V_S, I_S, V_{Cc} and I_C

The waveform of the overall simulation of reactive power diagram is shown in Fig. 6 and waveforms of V_S, I_S, V_{Cc} and I_C are shown in Fig. 7.

VI. Experiment Results

A. Environment Setting

APF is composed of DC/AC inverter, transducer with signal conditioning boards, DSP control board, IGBT drivers and DC-link capacitor. The DSP control board is based on a high-speed Digital Signal Processor (D.S.P)-TMS320F2812, which has high performances in the real-time control and motor/machine control. And the integral PWM outputs make it more suitable for inverter control [13] [15] . Additional signal conditioning circuits are designed to transfer the transducer output signals into a voltage range signal that can satisfy the requirements of the A/D conversion. And then the A/D signals are transmitted to the DSP controller for processing. When the PWM control is employed [12] , the DSP will generate trigger signals to control the output of the inverter. The experimental environment is built in laboratory and the photo is below.

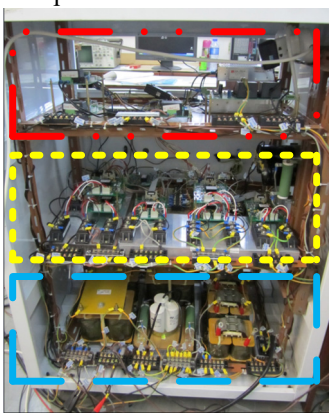

Fig. 8 The photos of a single phase adaptive HAPF experiment prototype

In Fig. 8, Several meters (load voltage meters, load current meters, coupling current meter, capacitor voltage meter and DC voltage meter) are set to have real-time monitor of the working states of the system. The power supply of control system is given by an individual 220V source voltage with isolated transformer for protection. Furtherly, the technical data of adaptive HAPF system is shown in Table VIII.

TABLE VIII TECHNICAL DATA OF ADAPTIVE HAPF SYSTEM

System Parameters	Value
Source voltage magnitude	55V/50Hz
Filtering inductance *Lc, Cc, C_{C1}, C_{C2}*	9.5 mH,41.0μF
DC-link reference voltage V_{dc}	20 V
PWM control	Hysteresis PWM (comparator period = 14.6kHz)
Load current THD Nonlinear Case	36.4%

B. Static Compensation Experimental Results

Fig. 9 shows the waveforms of source current I_S and voltage V_S, their THDs and spectrums taken by Fluke. The three cases are compared which are before compensation, after pure PF compensation and after adaptive HAPF compensation.

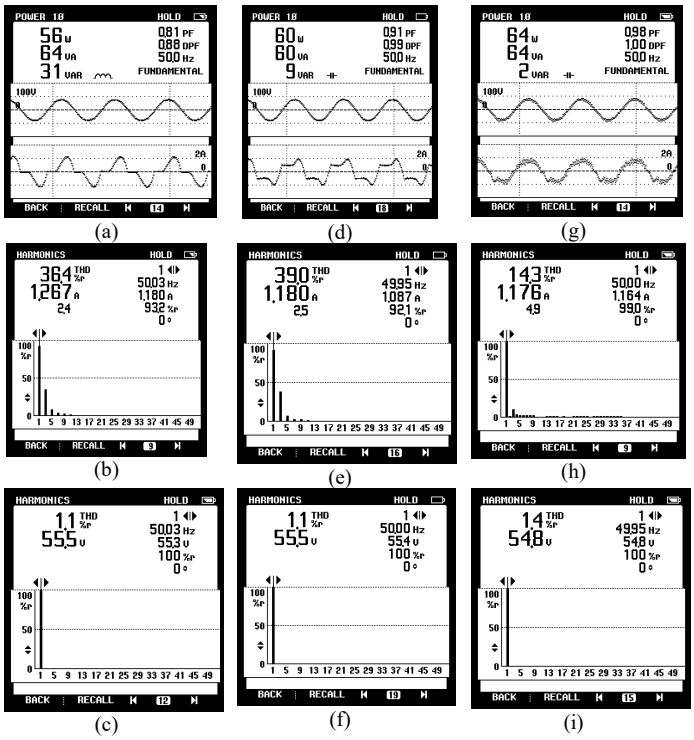

Fig. 9 The waveforms of source current Is and voltage Vs before compensation (a) power diagram (b) current spectrum (c) voltage spectrum; after pure passive filter compensation (d) power diagram (e) current spectrum (f) voltage spectrum; after adaptive HAPF compensation (g) power diagram (h) current spectrum (i) voltage spectrum;

C. Dynamic Compensation

The experimental system can adaptively respond to the changing of loading. The transient states during the loading change will be observed and the control strategy will be confirmed. All the experiment results in this section are obtained via Meridian Ultra PQ analyzer.

TABLE IX EXPERIMENTAL STEPS OF DYNAMIC COMPENSATION

Step	1	2	3	4
Mode of compensator	Initial state without compensation	Inductive load level 1	Inductive load level 2	Inductive load level 1
Step	5	6	7	
Mode of compensator	Capacitive load	Inductive load level 1	Initial state HAPF off	

The experiment in the hardware follows the same steps as the simulation which can be shown in Table IX The experimental system is tested under 55V. The power diagram of the load reactive power and source reactive power off the overall simulation is shown in Fig. 10.

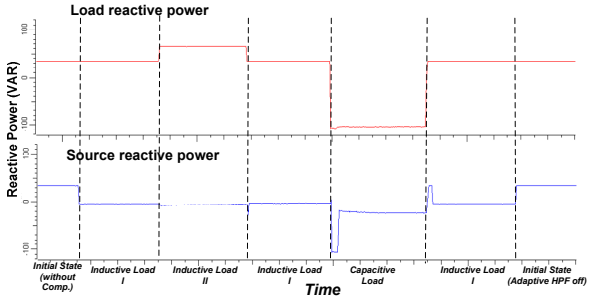

Fig. 10 Experiment results of source reactive power and load reactive power

From Fig. 10, it shows that the source reactive power can be compensated to almost zero after the turn on the adaptive HAPF which primarily proves the correctness and validity of the proposed adaptive HAPF.

D. Experiment of Transient States

The purposes of the transient experiment are to prove the proposed adaptive HAPF can dynamically switch the compensation mode without serious transient problems. The source voltage *Vs* (or load voltage V_{Load}), source current I_S, capacitor voltage V_{Cc} and compensating current I_C will be shown in different transient cases.

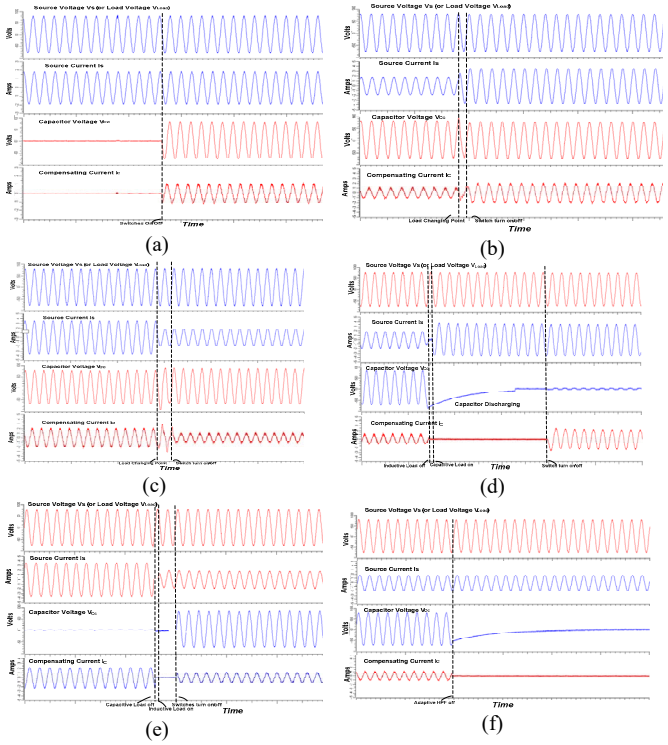

Fig. 11 The waveforms in experiment of transient states of V_S, I_S, V_{Cc} and I_C (a) when initial state change to inductive level I; (b) when inductive level I change to inductive level II (c) when inductive level II change to inductive level I; (d) when inductive level I change to capacitive load; (e) when inductive level I change to capacitive load; (f) when inductive level I change to initial state

Form the above Fig. 11, it can be seen that the adaptive HAPF can perform compensation dynamically without causing large transient problems. To be more exactly, there are no current or voltage overshooting problems (*dv/dt* or *di/dt*) and the peak value in transient state is much smaller than 3 times of it in steady state.

VII. Conclusions

In this paper, a reasonable structure of the adaptive hybrid active power filter (HAPF) is proposed for a single-phase low dc system. The reactive power and harmonics of the loads can be compensated dynamically, and the proposed HAPF has a low dc-linked voltage under both inductive and capacitive loading compensation. The capacitance and inductance in the passive part are calculated based on realistic example. The compensation range is deduced based on the capacitance and inductance in passive part. Transient analysis of the adaptive HAPF is studied. And the best switches turn-on/off time are found based on calculated and simulation results.

An experimental prototype of a single-phase adaptive HAPF was established and all the experimental results are consistent with the simulation results. All the simulation and experimental results satisfied the IEEE 519:1992 and IEC 61 000-3-2 standards. And the proposed adaptive HAPF can dynamicly compensate reactive power and current harmonics problem with a low dc-link voltage under both inductive and capacitive loading situations. Compared with the traditional APF for inductive loading compensation and HAPF for capacitive loading compensation, the proposed HAPF requires a low dc-linked voltage under both inductive and capacitive loading compensation, which can reduce the initial and operational costs.

References

[1] S. Srianthumrong and H. Akagi, "A medium-voltage transformerless ac/dc power conversion system consisting of a diode rectifier and a shunt hybrid filter," *IEEE Trans. Ind. Appl.,* vol. 39, no. 3, pp. 874–882, May/Jun. 2003.

[2] W. R. N. Santos, E. D. M. Fernandes, E. R. C. D. Silva, C. B. Jacobina, A. C. Oliveira, and P. M. Santos, "Transformerless single-phase universal active filter with UPS features and reduced number of electronic power switches," *IEEE Trans. Power Electron.*, vol. 31, no. 6, pp. 4111–4120, Jun. 2016.

[3] W. R. N. Santos et al., "The transformerless single-phase universal active power filter for harmonic and reactive power compensation," *IEEE Trans. Power Electron*., vol. 29, no. 7, pp. 3563–3572, Jul. 2014.

[4] S. Rahmani, A. Hamadi, N. Mendalek, and K. Al-Haddad, "A new control technique for three-phase shunt hybrid power filter," *IEEE Trans. Ind. Electron.*, vol. 56, no. 8, pp. 2904–2915, Aug. 2009.

[5] L. Wang, C. S. Lam, and M. C. Wong, "Modeling and parameter design of thyristor controlled LC-coupled hybrid active power filter (TCLC-HAPF) for unbalanced compensation," *IEEE Trans. Ind. Electron.*, 2017, to be published. doi: 10.1109/TIE.2016.2625239.

[6] J. Chen, X. Zhang, and C. Wen, "Harmonics attenuation and power factor correction of a more electric aircraft power grid using active power filter," *IEEE Trans. Ind. Electron.*, vol. 63, no. 12, pp. 7310–7319, Dec. 2016.

[7] L. Wang, C.-S. Lam, and M.-C. Wong, "A hybrid-STATCOM with wide compensation range and low DC-link voltage," *IEEE Trans. Ind. Electron*., vol. 63, no. 6, pp. 3333–3343, Jun. 2016.

[8] K.-J. Sun, "Thyristor control LC capacitance compensation circuit," Chinese Patent 201966624U, Sep. 7, 2011.

[9] S. E. Haque, N. H. Malik, and W. Shepherd, "Operation of a fixed capacitor-thyristor controlled reactor (FC-TCR) power factor compensator," *IEEE Trans. Power App. Syst.*, vol. PAS-104, no. 6, pp. 1385–1390, Jul. 1985

[10] A. Luo, Z. Shuai, W. Zhu, and Z. J. Shen, "Combined system for harmonic suppression and reactive power compensation," *IEEE Trans. Ind. Electron*., vol. 56, no. 2, pp. 418–428, Feb. 2009.

[11] L. Wang and K.-H. Wang, "Dynamic stability analysis of a DFIG-based offshore wind farm connected to a power grid through an HVDC link," *IEEE Trans. Power Syst*., vol. 26, no. 3, pp. 1501–1510, Aug. 2011.

[12] L. Wang, C.-S. Lam, and M.-C. Wong, "Hardware and software design of a low DC-link voltage and wide compensation range thyristor controlled LC-coupling hybrid active power filter," in Proc. Region Conf. (TENCON), Nov. 2015, pp. 1–4.

[13] IEEE Recommended Practices and Requirements for Harmonic Control in Electrical Power Systems, IEEE Standard 519-2014, 2014.

[14] L. Wang et al., "Non-linear adaptive hysteresis band pulse-width modulation control for hybrid active power filters to reduce switching loss," IET Power Electron., vol. 8, no. 11, pp. 2156–2167, Nov. 2015.

[15] M.-C. Wong et al., "Self-reconfiguration property of a mixed signal controller for improving power quality compensation during light loading," IEEE Trans. Power Electron., vol. 30, no. 10, pp. 5938–5951, Oct. 2015.